$\Delta(1232)$ isobar excitations in nuclear many-body systems derived from various NN interactions

T. Frick, S. Kaiser, and H. Müther
Institut für Theoretische Physik, Universität Tübingen, D-72076 Tübingen, Germany

A. Polls
Departament d'Estructura i Constituents de la Matèria, Universitat de Barcelona, E-08028 Barcelona, Spain
(Received 15 January 2001; published 8 June 2001)

Δ isobar components in the nuclear many-body wave function are investigated for the deuteron, light nuclei (^{16}O), and infinite nuclear matter within the framework of the coupled-cluster theory. The predictions derived for various realistic models of the baryon-baryon interaction are compared to each other. These include local (V28) and nonlocal meson exchange potentials (Bonn_{2000}) but also a model recently derived by the Salamanca group accounting for quark degrees of freedom. The characteristic differences which are obtained for the $N\Delta$ and $\Delta\Delta$ correlation functions are related to the approximation made in deriving the matrix elements for the baryon-baryon interaction.

DOI: 10.1103/PhysRevC.64.014309 PACS number(s): 21.60.−n, 21.65.+f, 21.30.−x

I. INTRODUCTION

It has always been one of the basic challenges of theoretical nuclear physics to derive the basic properties of nuclei from realistic models of the nucleon-nucleon (NN) interactions. Very sophisticated approximation schemes have been developed to solve the many-body problem of strongly interacting nucleons. As examples we mention Brueckner hole-line expansion [1], the coupled-cluster or ''exponential S'' approach [2], the self-consistent evaluation of Green's functions [3], variational approaches using chain summation (FHNC/SOC) methods [4], and recent developments employing quantum Monte Carlo techniques [5]. (See, e.g., the recent review [6] on these many-body approaches.)

A major ingredient for such investigations is the definition of a realistic NN interaction. Here we define a realistic NN interaction to be a model for the nucleon nucleon interaction in which the parameters have been adjusted to obtain a very good fit of the experimental NN scattering data at energies up to the threshold for π production. As examples for modern realistic interactions we refer the reader to Refs. [7–9].

The central assumption of such investigations is that the nucleons can be considered as inert particles interacting by two-body forces, which are identical in the vacuum and in the nuclear medium. It is of course well known that nucleons are not elementary particles. At short distances, nucleons will polarize each other, which will lead to virtual excitations. These subnucleonic degrees of freedom are effectively taken into account in the realistic NN interaction as the parameters are adjusted to the data.

As an example we mention the processes of the type that two nucleons interact with each other exchanging a π or ρ meson leading to a $N\Delta$ or $\Delta\Delta$ state [10]. After the exchange of a second meson the two baryons may be returned into a NN state such that this process contributes to the amplitude for elastic NN scattering. A theoretical approach which accounts for interacting nucleons only parametrizes this process with intermediate isobar excitations by adjusting, e.g., the coupling constant of the σ meson in a one-boson-exchange model for the NN interaction [11]. If, however, the isobar configurations are included explicitly one finds that a large part of the medium range attraction in the NN interaction originates from the coupling to the $N\Delta$ and $\Delta\Delta$ configurations.

Both kinds of models, with and without the explicit consideration of isobar configurations, yield essentially the interaction for two nucleons in the vacuum, since they are adjusted to reproduce the NN phase shifts. Remarkable differences show up, however, if the different kinds of interactions are considered for the interaction of two nucleons inside a nuclear medium. While the exchange of the σ meson is essentially the same in the vacuum and in the nuclear medium, the formation of virtual $N\Delta$ and $\Delta\Delta$ configurations is suppressed in nuclear matter (due to Pauli effects and binding of the nucleons) as compared to the vacuum. This leads to a loss of attraction for the effective interaction of two nucleons in the medium, which results in a smaller calculated binding energy. This effect has been investigated by various groups using the Brueckner-Hartree-Fock approximation, which means that correlations between nucleons are taken into account by means of the effective interaction, the G matrix [12–14].

The isobar degrees of freedom may of course also be considered explicitly in the solution of the nuclear many-body problem, i.e., one allows for many-body wave functions which contain isobar configurations. Such investigations have been made, e.g., for the three-nucleon problem [15,16] and for nuclear matter [14]. Presently, there is a renewed interest in the study of these isobar configurations in the nuclear wave function. One reason is the attempt to explore the isobar components in the nuclear wave function by means of different experiments. This includes the photoproduction of pions [17] and the isobar current contribution to exclusive $(e,e'NN)$ reactions [18]. Another reason is the development of new models for the baryon-baryon interaction including isobar configurations [19–21].

In this study we would like to investigate the predictions for the isobar components in the nuclear wave functions derived from various models for the baryon-baryon interaction. We are going to compare the isobar amplitudes calculated

for the Argonne V28 potential [19] with those derived from a recent update [21] of model I in Table B.1 of Ref. [22], which we will denote as Bonn_{2000}. Both of these models are based on the meson exchange picture of the baryon-baryon interaction. This means that, e.g., the transition potential $NN \to N\Delta$ is dominated by the contribution from π exchange. While the Bonn_{2000} approach considers the complete relativistic structure of this term, the V28 model reduces this π exchange contribution to a local potential. This π exchange contribution is supplemented by the ρ exchange in the Bonn_{2000} model. The V28 approach, on the other hand, adds a phenomenological contribution of short range. In Ref. [23] it has been observed that the reduction of meson exchange interactions to the local approximation yields characteristic differences. Can such differences also be observed for the isobar contributions?

A quite different approach has recently been developed by the Salamanca group [20]. They derive a NN interaction in the framework of the chiral quark cluster (CQC) model. The problem of two interacting clusters (baryons) of quarks is solved by means of the resonating group method. The Pauli principle between the interacting quarks is an important source for the short-range repulsion of the NN interaction [24]. At large distances the π exchange between the quarks in the two clusters evolves to the π exchange between two baryons. At shorter distances, however, this nonlocal model for the baryon-baryon interaction might yield results that are quite different from a meson-exchange picture. This Salamanca potential does not give such a perfect fit to the NN scattering phase shifts as the Bonn_{2000} or the V28. For the ${}^1S_0$ and ${}^3S_1 - {}^3D_1$ partial waves of the NN system, however, the agreement with the empirical data is rather good.

We are going to compare correlated two-baryon wave functions in the deuteron, ${}^{16}\text{O}$ and infinite nuclear matter derived from these three models of the baryon-baryon interaction. While the deuteron wave functions are obtained from an exact diagonalization in momentum space, the wave functions for ${}^{16}\text{O}$ and nuclear matter are calculated in the framework of the ''exponential S'' approach [2], generalized to include isobar degrees of freedom and evaluated in momentum representation.

After this introduction we discuss some differences between the transition potentials for V28 and Bonn_{2000} in the next section. The wave functions of the deuteron derived from these three models are compared in Sec. III, while the correlation functions for ${}^{16}\text{O}$ and infinite nuclear matter are presented in Sec. IV. A summary and conclusions are added in the final section.

II. TRANSITION POTENTIALS IN DIFFERENT MODELS

The key for an understanding of isobar components in the many-body wave function of nuclear systems is the transition potential, i.e., the matrix elements of the baryon-baryon interaction connecting two-nucleon states to $N\Delta$ and $\Delta\Delta$ configurations. A transition $N \leftrightarrow \Delta$ implies the change of both spin and isospin from $\frac{1}{2}$ to $\frac{3}{2}$. As isospin conservation has to be fulfilled at each vertex, such a transition requires the emission or absorption of an isovector meson, if one is considering a meson-exchange model for the baryon-baryon interaction. The most important isovector meson contributing to such transitions is of course the pion. The $\rho(770)$ has a considerable effect, too, but mainly for large momentum transfers between the interacting baryons.

In this section we would like to compare the one-pion-exchange (OPE) contribution as it is included in the Bonn_{2000} interaction with the corresponding term in the Argonne V28 interaction. As an example we consider the transition potential $NN \leftrightarrow \Delta\Delta$, in particular we will focus the attention to the central component as it shows up in ${}^3S_1$ partial waves. This OPE transition amplitude has been formulated in a helicity representation in which the quantization axis of the particle spins are the directions of the relative momenta $\mathbf{q}$ and $\mathbf{q}'$ for the initial and final state, respectively [25],

$$\begin{aligned}\langle \mathbf{q}' \Lambda_{N_1} \Lambda_{N_2} | V^\pi | \mathbf{q} \Lambda_{\Delta_1} \Lambda_{\Delta_2} \rangle &= \frac{4\pi}{(2\pi)^3} \frac{f^2_{N\Delta\pi}}{m^2_\pi} c(T) (q'_\mu - q_\mu)(q'_\nu - q_\nu) F^2_\pi(\mathbf{q}' - \mathbf{q}) \\ &\times \frac{\overline{u}(-\mathbf{q}', \Lambda_{N_2}) u^\mu(-\mathbf{q}, \Lambda_{\Delta_2}) \overline{u}(\mathbf{q}', \Lambda_{N_1}) u^\nu(\mathbf{q}, \Lambda_{\Delta_1})}{\sqrt{(\mathbf{q}' - \mathbf{q})^2 + m^2_\pi} [\sqrt{(\mathbf{q}' - \mathbf{q})^2 + m^2_\pi} + m_\Delta - m_N]}. \end{aligned} \tag{1}$$

$c(T)$ is the isospin factor that remains from isospin matrix elements and corresponds to $c(T) = -\sqrt{2}$ in this channel. The energy denominator in this expression contains the masses of the pion m_π, the nucleon m_N, and the m_Δ. It deviates from a simple pion-exchange propagator, as it has been derived from time-dependent perturbation theory accounting for the mass difference between m_N and m_Δ [26]. The function F_π represents the form factor for each $\pi N\Delta$ vertex. The initial relative momentum q and the final relative momentum q' are chosen along the z axis, $q = (0,0,q)$, and in the x-z plane, $q' = (0, q' \sin\theta, 0, q' \cos\theta)$, respectively, where θ is the angle between $\mathbf{q}$ and $\mathbf{q}'$. Λ_{B_i} labels the helicity quantum numbers of the spinors. For the Δ isobars these spinors fulfill the Rarita-Schwinger equations and can be constructed explicitly by coupling a vector field (spin 1) and a Dirac field (spin $\frac{1}{2}$)

$$u_\mu(\mathbf{q}, \Lambda) = \sum_{\lambda, s} C^{(3/2)\Lambda}_{1\lambda(1/2)s} e_\mu(\mathbf{q}, \lambda) u(\mathbf{q}, s), \tag{2}$$

with

$$e_\mu(\mathbf{q}, \lambda) = \left(\frac{\hat{\mathbf{e}}_\lambda \cdot \mathbf{q}}{m_\Delta}, -\hat{\mathbf{e}}_\lambda - \frac{\mathbf{q}(\hat{\mathbf{e}}_\lambda \cdot \mathbf{q})}{m_\Delta(\sqrt{\mathbf{q}^2 + m^2_\Delta} + m_\Delta)} \right), \tag{3}$$

where the $C^{(3/2)\Lambda}_{1\lambda(1/2)s}$ are Clebsch-Gordan coefficients in the notation of Ref. [27] and $u(\mathbf{p}, \mathbf{s})$ is a Dirac spinor in spin state s. $\hat{\mathbf{e}}_+$, $\hat{\mathbf{e}}_0$, and $\hat{\mathbf{e}}_-$ are the circular polarization vectors.

From both the Dirac spinors for the nucleons and the Rarita-Schwinger spinors for the deltas, the complex momentum structure is now removed by taking their value at $\mathbf{q} = \mathbf{q}' = 0$. It is straightforward to obtain the helicity Feyn-

man graph structure (1) for all $2\times2\times4\times4=64$ combinations of helicity projection numbers in this ''static'' approximation. Most of them can be derived from symmetry relations [25], and one only needs to evaluate ten matrix elements explicitly.

The helicity amplitudes are then projected onto states with definite total relative angular momentum J

$$\langle q' J^{\Lambda'} \Lambda_{N_1} \Lambda_{N_2} | V^\pi | q\, J^\Lambda \Lambda_{\Delta_1} \Lambda_{\Delta_2} \rangle = 2\pi \int_{-1}^{1} d(\cos\theta) d^J_{\Lambda,\Lambda'}(\theta) \langle \mathbf{q}' \Lambda_{N_1} \Lambda_{N_2} | V^\pi | \mathbf{q} \Lambda_{\Delta_1} \Lambda_{\Delta_2} \rangle. \tag{4}$$

Here, $d^J_{\Lambda,\Lambda'}(\theta)$ are the reduced rotation matrices with $\Lambda = \Lambda_{\Delta_1} - \Lambda_{\Delta_2}$ and $\Lambda' = \Lambda_{N_1} - \Lambda_{N_2}$. In the next step one performs the transformation into the basis of the partial wave states, in which orbital angular momentum L and spin S are coupled to J:

$$\begin{aligned}\langle q'\ {}^{2S'+1}L'^{NN}_J | V^\pi | q\ {}^{2S+1}L^{\Delta\Delta}_J \rangle &= \frac{\sqrt{(2L'+1)(2L+1)}}{2J+1} \\ &\times \sum_{\Lambda_{N_1}\Lambda_{N_2}\Lambda_{\Delta_1}\Lambda_{\Delta_2}} C^{J\Lambda'}_{L'0S'\Lambda'} C^{S'\Lambda'}_{(1/2)\Lambda_{N_1}(1/2)-\Lambda_{N_2}} \\ &\times \langle q' J^{\Lambda'} \Lambda_{N_1} \Lambda_{N_2} | V^\pi | q\, J^\Lambda \Lambda_{\Delta_1} \Lambda_{\Delta_2} \rangle \\ &\times C^{S\Lambda}_{(3/2)\Lambda_{\Delta_1}(3/2)-\Lambda_{\Delta_2}} C^{J\Lambda}_{L0S\Lambda}.\end{aligned} \tag{5}$$

The transformation coefficients have been taken from Ref. [28].

In order to compare these matrix elements for the transition potential in the Bonn_{2000} model with the corresponding one for the V28, we consider two approximations.

In evaluating the helicity amplitudes of Eq. (1) the nonrelativistic static limit is considered, i.e., the Dirac spinors as well as the Rarita-Schwinger are considered for $\mathbf{q}=\mathbf{q}'=\mathbf{0}$. The energy denominator in Eq. (1) is replaced by the usual pion propagator by ignoring the mass difference $m_\Delta - m_N$.

Using these approximations an analytical expression is obtained for

$$\langle q'\ {}^3S^{NN}_1 | V^\pi | q\ {}^3S^{\Delta\Delta}_1 \rangle = -\frac{4\pi^2}{(2\pi)^3} \frac{\sqrt{40}}{9} \frac{f^2_{N\Delta\pi}}{m^2_\pi} \int_{-1}^{1} d(\cos\theta) \times \left[1 - \frac{m^2_\pi}{(\mathbf{q}'-\mathbf{q})^2 + m^2_\pi} \right] F^2_\pi(\mathbf{q}'-\mathbf{q}) \tag{6}$$

that depends on the momentum transfer $\mathbf{q}'-\mathbf{q}$ only. This means that the interaction is local. Transforming this expression for the central part of the transition potential into configuration space, we can identify a Yukawa term and a contact term, both multiplied by the form factor.

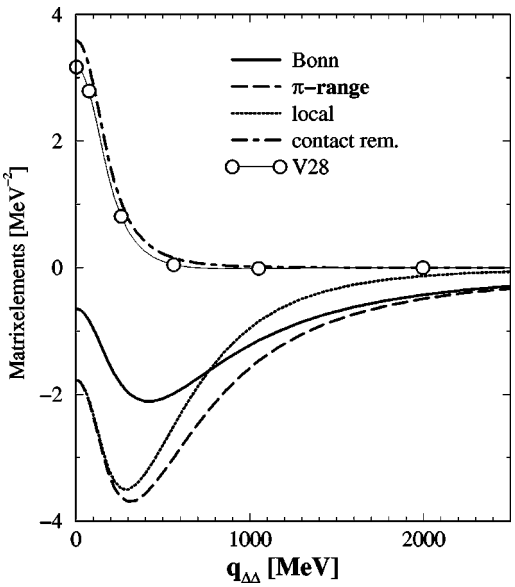

FIG. 1. Matrix elements for the one-pion exchange contribution to the transition potential $\langle q'\,{}^3S^{NN}_1 | V^\pi | q\ {}^3S^{\Delta\Delta}_1 \rangle$ assuming various approximations as discussed in the text. Results are displayed as a function of the momentum q in the $\Delta\Delta$ state. The momentum of the NN state has been fixed to $q=100$ MeV. All values have been multiplied with a common factor of 10^6.

This expression can be compared with the local transition potential as defined for the Argonne V28 interaction

$$\langle r\ {}^3S^{NN}_1 | V^\pi | r\ {}^3S^{\Delta\Delta}_1 \rangle = \left(\frac{f^2_{N\Delta\pi} m_\pi}{12\pi} \right) \frac{e^{-m_\pi r}}{m_\pi r} (1 - e^{-cr^2}) \times \langle {}^3S^{NN}_1 | (\mathbf{S}_1\mathbf{S}_2)^\dagger (\mathbf{T}_1\mathbf{T}_2)^\dagger | {}^3S^{\Delta\Delta}_1 \rangle, \tag{7}$$

with $\mathbf{S}_i$ and $\mathbf{T}_i$ denoting the transition operator for spin and isospin. Note that comparing this expression with the local approximation to the Bonn_{2000} model in Eq. (6), the contact term is removed and the form factor is replaced in V28 by a Gaussian cutoff to regularize the matrix elements for small interparticle distances.

Matrix elements of the one-pion-exchange (OPE) contribution to the transition potential in the partial wave $\langle q'\ {}^3S^{NN}_1 | V^\pi | q\ {}^3S^{\Delta\Delta}_1 \rangle$ for these different approaches are displayed in Fig. 1. The relative momentum of the NN pair q' is fixed at 100 MeV and the matrix elements are presented as a function of the relative momentum for the $\Delta\Delta$ state.

The mass difference $m_\Delta - m_N$ in the pion propagator of Eq. (1) has a remarkable effect on the calculated transition potential. This can be seen in Fig. 1 from the comparison of the solid line (Bonn), which represents the complete OPE contribution in the Bonn_{2000} potential, with the long dashed line (π range), which exhibits the results obtained after replacing the pion propagator of Eq. (1) by the conventional π propagator. The inclusion of the mass difference $m_\Delta - m_N$ leads to a quenching of the transition potential by about a factor two for small momenta, while the two curves approach each other at large values of $q_{\Delta\Delta}$. This means that

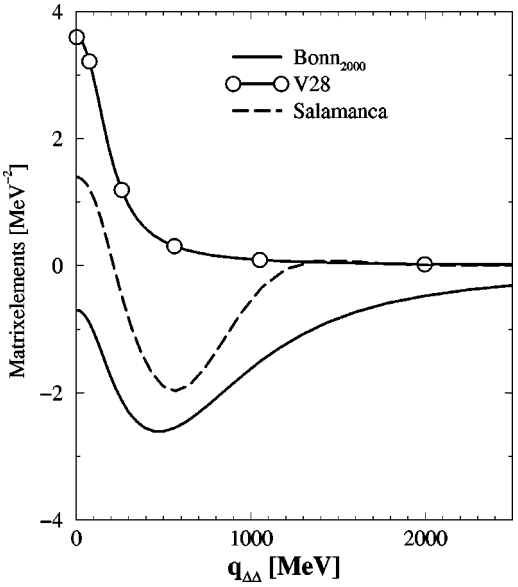

FIG. 2. Matrix elements for the transition potential $NN \to \Delta\Delta$ in the $^3S_1$ central partial wave assuming the Bonn_{2000}, Argonne V28, and Salamanca quark model approaches. For further details see Fig. 1.

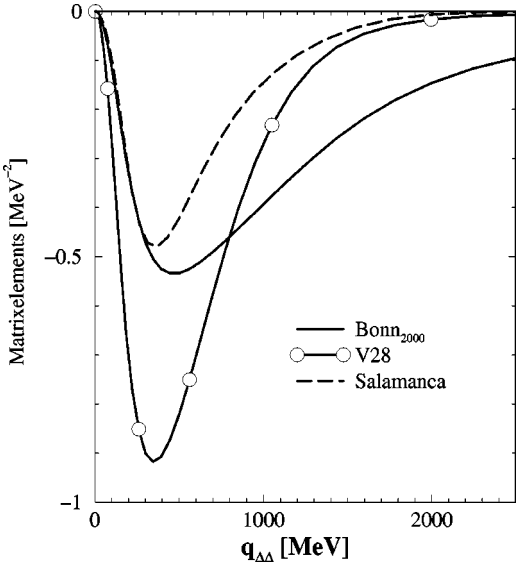

FIG. 3. Matrix elements for the transition potential $\langle q'^3S_1^{NN}|V|q\ ^7D_1^{\Delta\Delta}\rangle$ assuming the Bonn_{2000}, Argonne V28, and Salamanca quark model approaches. For further details see Fig. 1.

the inclusion of the mass difference leads to a transition potential that is generally weaker and of shorter range, a feature which has already been observed, e.g., in Ref. [29].

If one furthermore employs the nonrelativistic limit, one obtains the local representation of the OPE of Eq. (6), which is given in Fig. 1 by the dashed line (local). The removal of the relativistic features yields a sizable effect at larger momenta in particular. The dashed-dotted line (contact rem.) results from the expression of Eq. (6) if the contact term, the constant in the momentum representation, is ignored. The removal of this contact term has a very strong effect on the transition potential in this central partial wave with $l=0$. Only after removing this contact term, we obtain an OPE component of the Bonn potential, which is essentially identical to the OPE contribution in the Argonne V28 model.

The comparison of these various approximations in Fig. 1 makes it rather obvious that the different treatment of the OPE contribution to the $NN \to \Delta\Delta$ transition potential leads to quite different matrix elements in the relativistic Bonn model, defined in momentum space, as compared to the local treatment in the Argonne V28. This OPE contribution is the most important ingredient to the transition potential in both models. The addition of the ρ exchange in the case of the Bonn_{2000} model leads to minor although non-negligible modifications. This can be seen from the comparison of Fig. 1 with Fig. 2, which shows matrix elements of the total transition potential. In addition to the results for the Bonn_{2000} and V28 models, this figure also shows the corresponding values for the quark model of the Salamanca group [20]. We see again the huge differences between the V28 and the Bonn_{2000} model, which even lead to a difference in sign. From our discussion above we know that the main part of differences can be traced back to the different treatment of the OPE contribution.

The Salamanca chiral quark cluster (CQC) model, which we study as a third example [20] cannot be considered as an entirely realistic potential because it does not fit the *P*-phase shifts for *NN* scattering with good accuracy; the phase shifts in the $^1S_0$ and $^3S_1 - {}^3D_1$ channels are reproduced very well, however. In the CQC model, the long-range interaction is generated by OPE as well. In the core region, the potential is determined by gluon exchange and the Pauli principle. The latter requires total antisymmetry of the six-quark wave function and this leads to a dependence of the baryon-baryon potential on the initial kinetic energy E_{in} of two interacting nucleons. For the results displayed in Fig. 2 we assume a value $E_{in}=0$ for this energy.

The matrix elements for the transition potential of the Salamanca model exhibit values in between the two approaches discussed above. The shape is similar to the one of the Bonn potential, however, approaching the value of zero with increasing momenta much faster than the Bonn potential. This might be an indication that the Pauli effects in the quark model provide a much stronger cutoff at high momenta than the form factor used in the Bonn potential.

As another example we compare results obtained for these three models also for the case $\langle q'^3S_1^{NN}|V|q\ ^7D_1^{\Delta\Delta}\rangle$ in Fig. 3. The differences between Bonn_{2000} and V28 can again be traced back to the different treatment of the OPE. For this partial wave, however, one does not obtain any contact term contribution. This implies that the V28 is stronger at small momenta as it ignores the mass difference $m_\Delta - m_N$ in the pion propagator and weaker than Bonn_{2000} at high momenta because of the nonlocalities included in the Bonn model. The matrix elements for the Salamanca model are similar to those of the Bonn_{2000} potential at small momenta but exhibit features of a stronger cutoff at high momenta.

III. THE WAVE FUNCTIONS OF THE DEUTERON

Solutions of the bound state two-particle problem have been obtained for the Argonne V28, the Bonn_{2000}, and the

TABLE I. Contributions to the kinetic and potential energy of the deuteron originating from the different parts of the wave function. The kinetic energy T_{total} is the sum of the kinetic energies originating from the NN wave function in $^3S_1$ (T_S^N) and $^3D_1$ (T_D^N) partial waves plus the kinetic energy (T^Δ) from the $\Delta\Delta$ components. The term T^Δ also accounts for the $N\Delta$ mass difference. The potential energy contains contributions from the various parts of the $NN \to NN$ potential (V^{NN}), the $NN \to \Delta\Delta$ terms ($V^{N\Delta}$), and the $\Delta\Delta \to \Delta\Delta$ terms ($V^{\Delta\Delta}$). Results are given for the three models with isobar configurations. Note that the interaction model Bonn_{2000} does not consider any $V^{\Delta\Delta}$ interaction terms. For comparison we also show results from pure nucleonic interaction models V14 and CD-Bonn. All entries are given in MeV.

	Arg. V28	Bonn_{2000}	Sal. CQC	Arg. V14	CD-Bonn
T_{total}	23.75	22.29	17.82	19.22	15.48
V_{total}	−25.97	−24.51	−20.04	−21.44	−17.70
T_S^N	10.32	10.25	10.84	10.54	9.79
T_D^N	8.95	5.35	5.13	8.68	5.69
T^Δ	4.48	6.69	1.85		
V_{SS}^{NN}	7.08	1.52	−5.67	−1.83	−4.77
V_{DD}^{NN}	5.86	1.80	0.70	1.99	1.34
V_{SD}^{NN}	−29.22	−14.38	−11.64	−21.60	−14.27
$V^{N\Delta}$	−10.40	−13.44	−3.16		
$V^{\Delta\Delta}$	0.71		−0.28		

Salamanca CQC potential. The nucleonic part of the deuteron wave function contains components $^3S_1 - {}^3D_1$ partial waves. If Δ degrees of freedom shall be taken into account explicitly, one has to extend the two coupled nucleonic channels by four $\Delta\Delta$ partial waves, namely, $^3S_1^{\Delta\Delta}$, $^3D_1^{\Delta\Delta}$, $^7D_1^{\Delta\Delta}$, and $^7G_1^{\Delta\Delta}$. No $N\Delta$ states can occur because the deuteron is an isospin $T=0$ state and the isospins of N and Δ cannot couple to zero. The problem to determine the baryonic wave function in the 6 coupled channels has been solved in a spherical box with radius $R_{\text{box}}=20$ fm. The spherical Bessel functions with the boundary condition

$$j_l(k_{il}R_{\text{box}})=0$$

can be used to construct a complete basis of orthonormalized states for the bound state wave functions within the spherical box [30]. The coupled channel Hamiltonian was calculated in this basis of momentum eigenstates of the box and diagonalized numerically. Up to 300 discrete momenta were needed to get stable results for the binding energy. The results for energies and the wave functions obtained with the Argonne V28 and for the Salamanca potential are in good agreement with the values given in Refs. [19] and [20], respectively.

All NN interactions, which we consider, are adjusted to fit the total energy of the deuteron, which can be written as a sum of the kinetic energy T_{total} and potential energy V_{total} with

$$\begin{aligned} T_{\text{total}} &= \langle NN\ {}^3S_1|T|NN\ {}^3S_1\rangle + \langle NN\ {}^3D_1|T|NN\ {}^3D_1\rangle \\ &\quad + \langle \Delta\Delta|T|\Delta\Delta\rangle \\ &= T_S^N + T_D^N + T^\Delta. \end{aligned} \tag{8}$$

Note that the term T^Δ sums up the kinetic energy from all partial wave components in the $\Delta\Delta$ wave function and includes the contribution from the $N-\Delta$ mass difference. The potential energy can be split into

$$\begin{aligned} V_{\text{total}} &= \langle NN\ {}^3S_1|V|NN\ {}^3S_1\rangle + \langle NN\ {}^3D_1|V|NN\ {}^3D_1\rangle \\ &\quad + 2\langle NN\ {}^3S_1|V|NN\ {}^3D_1\rangle + 2\langle NN|V|\Delta\Delta\rangle \\ &\quad + \langle \Delta\Delta|V|\Delta\Delta\rangle = V_{SS}^{NN} + V_{DD}^{NN} + V_{SD}^{NN} + V^{N\Delta} + V^{\Delta\Delta}. \end{aligned} \tag{9}$$

The contributions of these various terms to the energy of the deuteron are listed in Table I, while the norm of the various partial wave contributions to the wave function are presented in Table II for the three interaction models with

TABLE II. Probability for D state and $\Delta\Delta$ components in the deuteron for different models of the baryon-baryon interaction. All entries in percent.

%	V28	Bonn_{2000}	CQC
$^3S_1^{NN}$	93.341	94.685	95.199
$^3D_1^{NN}$	6.133	4.705	4.567
$^3S_1^{\Delta\Delta}$	0.043	0.223	0.107
$^3D_1^{\Delta\Delta}$	0.020	0.022	0.004
$^7D_1^{\Delta\Delta}$	0.417	0.361	0.124
$^7G_1^{\Delta\Delta}$	0.045	0.005	0.006
Total $\Delta\Delta$	0.524	0.611	0.241

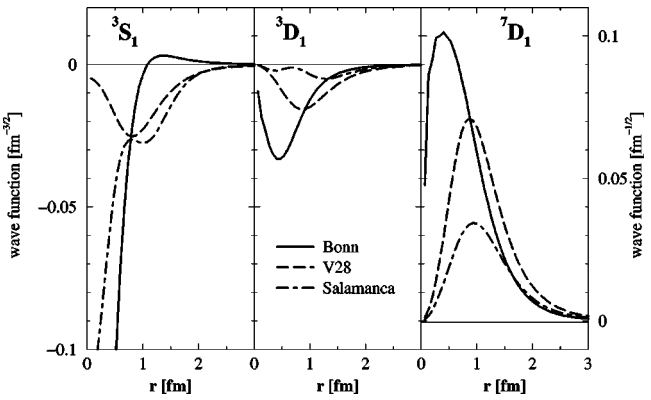

FIG. 4. Isobar components in the deuteron wave function using the three different models for the baryon-baryon interaction. The scale on the left-hand side of the figure refers to the left and middle graph, while the scale on the right-hand side refers to the right part only.

inclusion of isobars. For a comparison Table I also shows the result for two *NN* interaction models without the explicit treatment of isobar configurations: the Argonne potential model V14 [19] and the charge-dependent Bonn potential [7].

Although the sum of these various energy contributions yields the same energy of the deuteron for all the interaction models, there are remarkable differences in the individual terms. The inclusion of isobar components in the wave function yields a contribution to the binding energy of -5.21, -6.75, and -1.59 MeV for the V28, the Bonn_{2000} and the Salamanca interaction, respectively. This means that V28 and Bonn_{2000} predict an unbound deuteron, if the $\Delta\Delta$ components in the wave function would be suppressed, while the Salamanca interaction leads to a much weaker contribution of the isobar configurations. These differences also show up in the norm of the various partial wave components in the deuteron wave function listed in Table II. Comparing these occupation probabilities one finds that all interactions predict the largest contribution to the $\Delta\Delta$ probability in the $^7D_1$ partial wave. The largest probability for this partial wave is obtained for the V28 potential, while Bonn_{2000} and the Salamanca interaction in particular yield much smaller probabilities in this channel. The origin of these differences can be deduced from Fig. 4, which exhibits the $\Delta\Delta$ wave functions. The Argonne potential leads to a wave function in the $^7D_1$, $\Delta\Delta$ channel, which is of longer range than those derived from the other two interactions. The main reason for this feature is the fact that the OPE contribution to the $NN \rightarrow \Delta\Delta$ transition potential neglects the $N-\Delta$ mass difference in the pion propagator [see Eq. (1)], which leads to a transition potential of longer range. Comparing the wave functions in this channel derived from the Bonn_{2000} and the Salamanca interaction, one observes that the latter is strongly suppressed at short relative distances as compared to the former, which supports the argument presented already in the comparison of the matrix elements of the interaction, that the quark model leads to a much stronger effective cutoff at short distances than the cutoffs used in the meson exchange model.

The most significant difference in the predictions for the isobar components of the wave function can be seen in the $^3S_1$, $\Delta\Delta$ channel. While the Bonn and Salamanca models yield occupation probabilities, which are of similar size as those for the $^7D_1$, $\Delta\Delta$ channel, the probability for this channel derived from the V28 potential is much weaker. A qualitative difference can also be observed from the inspection of the wave function in this channel (see Fig. 4). The wave function obtained for the Bonn and Salamanca potential show a maximal amplitude for $r \rightarrow 0$, while the corresponding wave function deduced from the V28 potential is suppressed at small relative distances. These differences in the wave function reflect the fact that the contact term in the OPE contribution to the transition potential [see Eq. (6) and discussion there] is removed in the local representation of the OPE in V28, while the nonlocal representation of the OPE in the other models keeps a strong short range component.

The comparison of the $\Delta\Delta$ components in the deuteron wave function therefore reflects the main differences between the local approximation of the V28 and the nonlocal approaches of the Bonn and Salamanca model: The V28 contains a OPE component of longer range and suppresses the short range components much stronger than the other two models. Furthermore, the quark model approach leads to a stronger reduction than the typical cutoff that is used in the meson exchange models of the Bonn group. This leads to much weaker $\Delta\Delta$ components in the deuteron wave function for the Salamanca model.

It is worth noting that the contributions of V_{SD}^{NN} to the potential energy of the deuteron (see Table I) are significantly larger for the local Argonne potentials V14 and V28, than for the various versions of the Bonn potential and the Salamanca potential. This observation suggests that the local representation of the tensor components of the *NN* interaction, in particular the contribution originating from π exchange yields matrix elements which are significantly larger than those evaluated within the nonlocal approaches (see also Refs. [23,31]).

IV. CORRELATIONS IN NUCLEAR MATTER AND ^{16}O

The wave functions of many-body systems are studied in the framework of the coupled-cluster theory [2]. In the coupled-cluster approach one starts assuming an appropriate Slater determinant Φ and writes the exact eigenstate Ψ for the *A*-particle system as

$$\Psi = e^S \Phi, \tag{10}$$

with *S* an operator of the form

$$S = \sum_{n=1}^{A} S_n, \tag{11}$$

where S_n is an *n*-particle operator which can be written for the case of $n=2$

$$S_2 = \frac{1}{4} \sum_{\nu_1,\nu_2,\rho_1,\rho_2} \langle \rho_1 \rho_2 | S_2 | \nu_1 \nu_2 \rangle a_{\rho_1}^\dagger a_{\rho_2}^\dagger a_{\nu_2} a_{\nu_1}. \tag{12}$$

In this equation $a^{\dagger}_{\rho_i}$ stand for fermion creation operators in states which are unoccupied in Φ, while a_{ν_i} represent annihilation operators for the nucleon single-particle states which are occupied in the Slater determinant Φ. Note that the $a^{\dagger}_{\rho_i}$ may also represent the creation of Δ isobar states. Therefore the S_2 amplitudes describe two-particle two-hole excitations relative to Φ but also $N\Delta$ and $\Delta\Delta$ excitations.

For our present investigation of nuclear matter we will assume Φ to be the Slater determinant defined in terms of plane waves, occupying all states with momenta up to the Fermi momentum $k_F = 1.36$ fm^{-1}. As an example for a finite nucleus, we will also consider ^{16}O. In this case we will assume Φ to be the Slater determinant, defined in terms of harmonic oscillator states ($\hbar\omega = 14$ MeV) with nucleons occupying the states of $0s$ and the $0p$ shell. If one assumes that these single-particle states represent an optimal single-particle basis, i.e., the amplitudes S_1 in Eq. (11) vanish, and ignores the contributions of linked n-particle correlations with $n \geqslant 3$ ($S_n = 0$ for $n \geqslant 3$), one obtains integral equations for amplitudes

$$\langle b_1 b_2 [k(lS)j] KLJ\tau | S_2 | (\nu_1\nu_2) J\tau \rangle, \tag{13}$$

which are solved in momentum space [32]. In this representation $b_1 b_2$ stand for NN, $N\Delta$, and $\Delta\Delta$ states, $k(lS)j$ denote the momentum, spin, and orbital quantum numbers for the partial wave basis of the relative motion of the two baryons. K and L represent the center of mass state and J and τ refer to the total angular momentum and isospin of the pair of baryons.

The S_2 amplitudes can be considered as correlation functions describing the difference between the correlated and uncorrelated wave function of two particles in the nuclear medium. As the uncorrelated Slater determinant Φ in Eq. (10) does not contain any isobar components, the S_2 amplitudes can be interpreted directly as the $N\Delta$ and $\Delta\Delta$ component of the two-particle wave function, if $b_1 b_2$ in Eq. (13) refers to $N\Delta$ and $\Delta\Delta$ states.

As typical examples for these correlation functions in nuclear matter, the $\Delta\Delta$ components for the relative wave function of two baryons in a state with isospin $\tau = 0$ and angular momentum $j = 1$ are given in Fig. 5. These components correspond to the components of the deuteron wave function in the same partial waves displayed in Fig. 4. In fact, these isobar components of the wave function for a pair of baryons in nuclear matter is very similar to the deuteron wave function if one compares the partial wave with $l = 2$. The $\Delta\Delta$ wave functions exhibit a tail of longer range in the case of the Argonne V28 interaction, which reflects the longer range of the $NN \rightarrow \Delta\Delta$ transition potential for this interaction as compared to the other two approaches. The Salamanca CQC approach yields amplitudes for these D waves which are considerably smaller. All these amplitudes are enhanced as compared to the deuteron wave function, which reflects the larger density of the nuclear matter system.

The situation is a little bit different if one compares the $^3S_1$, $\Delta\Delta$ component of the nuclear matter wave function with the corresponding part of the deuteron wave function.

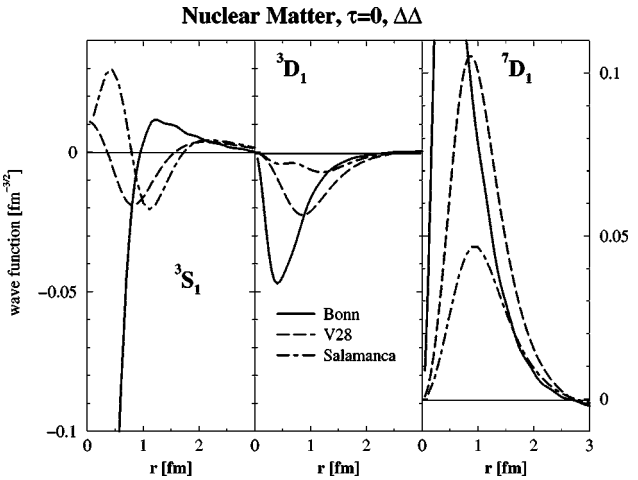

FIG. 5. Isobar components in the relative wave functions of two particles in nuclear matter with isospin $\tau = 0$ and $j = 1$. The scale on the left-hand side of the figure refers to the left and middle graph, while the scale on the right-hand side refers to the right part only.

The results obtained for the V28 and the Bonn potential yield wave functions of rather similar shape in the deuteron and in nuclear matter also for this channel. The wave functions derived from the Salamanca CQC interaction are rather different in nuclear matter as compared to the deuteron. At short distances they even have a different sign. This reflects a large nonlocality or momentum dependence of the short range component for the $NN \rightarrow \Delta\Delta$ transition potential derived in the CQC model.

In the nuclear many-body systems one also observes bound states of two baryons in states with isospin $\tau = 1$. As an example of such configurations we discuss $N\Delta$ and $\Delta\Delta$ components of two-particle wave functions in ^{16}O as displayed in Fig. 6. The comparison of the results obtained for the different interaction models leads to observations which are rather similar to those discussed for the states with $\tau = 0$ above. The difference in the range of the transition potentials $NN \rightarrow N\Delta$ for V28 and the other two interactions is not as significant as in the case of the $NN \rightarrow \Delta\Delta$ [compare the discussion of the propagator in Eq. (1)], which leads to smaller differences in the tail of the $^5D_0$ $N\Delta$ wave function than in the corresponding $\Delta\Delta$ state. A very significant model dependence is obtained in the $^1S_0$, $\Delta\Delta$ wave function.

The isobar-isobar relative wave functions derived for nuclear matter and finite nuclei are rather similar. Therefore we display only one of these examples for each channel. This demonstrates that isobar admixtures correspond to correlations in the many-body wave function which are of short range. Therefore they are not very sensitive to surface effects in finite nuclei and a local density approximation should be appropriate to consider isobar effects in finite nuclei.

V. CONCLUSIONS

Three different models for the baryon-baryon interaction, which fit NN scattering data and explicitly account for isobar degrees of freedom have been considered. These are the local

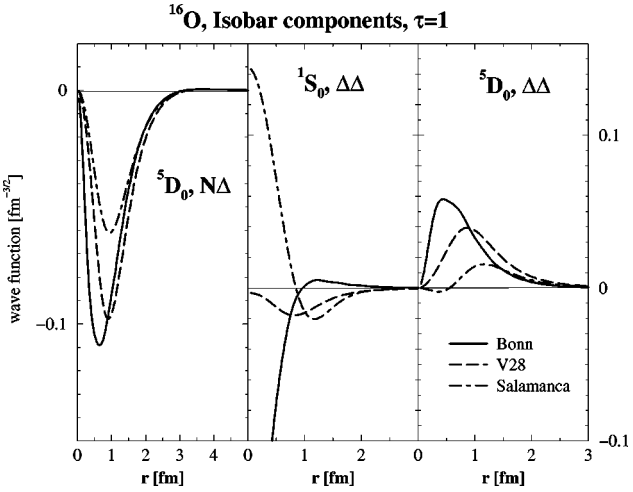

FIG. 6. Isobar components in the relative wave functions of two particles in ^{16}O with isospin $\tau=1$ and $j=0$. The uncorrelated state corresponds to two nucleons in the $0s_{1/2}$ state. The scale on the left-hand side of the figure refers to the left section of this figure only, while the scale on the right-hand side must be considered for the middle and the right section of this figure.

Argonne V28 potential [19], the Bonn$_{2000}$ [21] interaction model based on the relativistic meson exchange model, and an interaction based on the chiral quark cluster (CQC) model which has recently been developed by the Salamanca group [20]. The isobar components in the wave function of the deuteron and nuclear many-body systems including nuclear matter and ^{16}O as an example for a finite nucleus are evaluated. Significant differences are observed in the predictions from these models. These differences can be related to the assumptions made in determining the transition potential between NN, $N\Delta$, and $\Delta\Delta$ states. The V28 interaction model yields isobar wave functions of longer range than the other two. This can be traced back to the approximations which are made in reducing the π exchange contribution of the transition potentials to a local form. The most significant differences are observed in partial waves with $l=0$ at small distances. A main source of the discrepancies in these partial waves is related to a removal of a contact term in the local interaction model. The Bonn$_{2000}$ and Salamanca CQC model in particular exhibit important nonlocal features for the short range part of the interaction model. The Salamanca model predicts rather small isobar components in the nuclear many-body wave function. These different predictions for the isobar components in the many-body wave function could be very useful in distinguishing between different interaction models.

ACKNOWLEDGMENTS

We thank D. Entem for providing us with the Salamanca CQC potential and for useful discussions. We would also like to thank Francesca Samarucca and Ruprecht Machleidt for useful discussions. One of the authors (T.F.) would also like to thank the Dr.-Carl-Duisberg-Stiftung for supporting this work by a grant that enabled a stay at the Departament d'Estructura i Constituents de la Matèria in Barcelona, Spain. We would like also to acknowledge financial support from DGICYT (Spain) under Contract No. PB98-1247 and from Generalitat de Catalunya under Grant No. SGR2000-24.

[1] J. P. Jeukenne, A. Legeunne, and C. Mahaux, Phys. Rep. **25**, 83 (1976).
[2] H. Kümmel, K. H. Lührmann, and J. G. Zabolitzky, Phys. Rep. **36**, 1 (1978).
[3] W. H. Dickhoff and H. Müther, Rep. Prog. Phys. **11**, 1947 (1992).
[4] A. Akmal and V. R. Pandharipande, Phys. Rev. C **56**, 2261 (1997).
[5] J. Carlson and S. Schiavilla, Rev. Mod. Phys. **70**, 743 (1998).
[6] H. Müther and A. Polls, Prog. Part. Nucl. Phys. **45**, 243 (2000).
[7] R. Machleidt, F. Sammarruca, and Y. Song, Phys. Rev. C **53**, R1483 (1996).
[8] R. B. Wiringa, V. G. J. Stoks, and R. Schiavilla, Phys. Rev. C **51**, 38 (1995).
[9] V. G. J. Stoks, R. A. M. Klomp, C. P. F. Terheggen, and J. J. de Swart, Phys. Rev. C **49**, 2950 (1994).
[10] H. J. Weber and H. Arenhövel, Phys. Rep. **36**, 277 (1978).
[11] R. Machleidt, K. Holinde, and Ch. Elster, Phys. Rep. **149**, 1 (1987).
[12] A. M. Green, Rep. Prog. Phys. **39**, 1109 (1976).
[13] M. R. Anastasio, A. Faessler, H. Müther, K. Holinde, and R. Machleidt, Phys. Rev. C **18**, 2416 (1978).
[14] W. Manzke and M. Gari, Nucl. Phys. **A312**, 457 (1978).
[15] W. Streuve, C. Hajduk, P. U. Sauer, and W. Theis, Nucl. Phys. **A465**, 651 (1987).
[16] A. Picklesimer, R. A. Rice, and R. Brandenburg, Phys. Rev. C **44**, 1359 (1991); **46**, 1178 (1992).
[17] G. M. Huber *et al.*, Phys. Rev. C **62**, 044001 (2000).
[18] S. Boffi, C. Giusti, F. D. Pacati, and M. Radici, *Electromagnetic Response of Atomic Nuclei* (Oxford University Press, Oxford, 1996).
[19] R. B. Wiringa, R. A. Smith, and T. L. Ainsworth, Phys. Rev. C **29**, 1207 (1984).
[20] D. R. Entem, F. Fernández, and A. Valcarce, Phys. Rev. C **62**, 034002 (2000).
[21] R. Machleidt (unpublished).
[22] R. Machleidt, Adv. Nucl. Phys. **19**, 189 (1989).
[23] H. Müther and A. Polls, Phys. Rev. C **61**, 014304 (2000).
[24] A. Valcarce, A. Buchmann, F. Fernández, and Amand Faessler, Phys. Rev. C **51**, 1480 (1995).
[25] K. Holinde and R. Machleidt, Nucl. Phys. **A280**, 429 (1977).
[26] J. W. Durso, M. Saarela, G. E. Brown, and A. D. Jackson, Nucl. Phys. **A278**, 445 (1977).
[27] D. A. Varshalovich, A. N. Moskalev, and V. K. Khersonskii, *Quantum Theory of Angular Momentum* (World Scientific, Singapore, 1988).
[28] M. Jacob and G. C. Wick, Ann. Phys. (N.Y.) **7**, 404 (1959).

[29] K. Holinde, R. Machleidt, M. R. Anastasio, A. Fässler, and H. Müther, Phys. Rev. C **18**, 870 (1978).
[30] H. Müther, A. Polls, and W. H. Dickhoff, Phys. Rev. C **51**, 3040 (1995).
[31] A. Polls, H. Müther, R. Machleidt, and M. Hjorth-Jensen, Phys. Lett. B **432**, 1 (1998).
[32] C. Giusti, H. Müther, F. D. Pacati, and M. Stauf, Phys. Rev. C **60**, 054608 (1999).